ANTIMICROBIAL AGENTS AND CHEMOTHERAPY, Sept. 1994, p. 2125–2133
0066-4804/94/$04.00+0

Vol. 38, No. 9

Investigation of Ciprofloxacin Penetration into *Pseudomonas aeruginosa* Biofilms

P. A. SUCI,[1]* M. W. MITTELMAN,[2] F. P. YU,[1] AND G. G. GEESEY[1]

Center for Biofilm Engineering, Montana State University, Bozeman, Montana 59717,[1] and Centre for Infection and Biomaterials Research, Toronto Hospital, Toronto, Ontario, Canada M5G 2C4[2]

Received 12 October 1993/Returned for modification 13 April 1994/Accepted 25 June 1994

Bacterial infections associated with indwelling medical devices often demonstrate an intrinsic resistance to antimicrobial therapies. In order to explore the possibility of transport limitation to biofilm bacteria as a contributing factor, the penetration of a fluoroquinolone antibiotic, ciprofloxacin, through *Pseudomonas aeruginosa* biofilms was investigated. Attenuated total reflection Fourier transform infrared (ATR/FT-IR) spectrometry was employed to monitor bacterial colonization of a germanium substratum, transport of ciprofloxacin to the biofilm-substratum interface, and interaction of biofilm components with the antibiotic in a flowing system. Transport of the antibiotic to the biofilm-substratum interface during the 21-min exposure to 100 μg/ml was found to be significantly impeded by the biofilm. Significant changes in IR bands of the biofilm in regions of the spectrum associated with RNA and DNA vibrational modes appeared following exposure to the antibiotic, indicating chemical modification of biofilm components. These results suggest that transport limitations may be an important factor in the antimicrobial resistance of biofilm bacteria and that ATR/FT-IR spectrometry may be used to follow the time course of antimicrobial action in biofilms in situ.

Infections associated with implanted devices are notoriously difficult to treat and often lead to serious complications (6, 16, 21). Both cellular immunity mediated by phagocytic cells and complement-mediated opsonic factors have been found to be markedly reduced in proximity to a foreign body; therefore, significantly lower doses of the infecting agent(s) are required to initiate infection in the presence of an implant (10, 47). In addition, bacteria associated with surfaces are afforded a measure of protection from a variety of antagonistic agents including antibiotics (22, 45, 48). In situ studies have indicated that biofilm bacteria can sometimes withstand many times the dosage of antibiotic sufficient to completely eradicate planktonic organisms (2–4, 33, 34).

Relatively slow growth rate (18) and production of antibiotic-degrading enzymes (20) have both been implicated as contributing to antibiotic resistance of biofilm bacteria. Biofilm bacteria are typically embedded in a matrix of extracellular polymeric substances (11, 12). In addition to facilitating bacterial adhesion to device surfaces, extracellular polymeric substances may also impede antimicrobial penetration and impair opsonization (10). A reduction in the rate of antibiotic penetration of antibiotics into biofilm bacterial cells may provide cells sufficient time to switch on the expression of antibiotic-degrading enzymes. It may even be possible that some portions of a biofilm remain completely inaccessible to the antibiotic, even at high dose levels.

Previous studies have established the utility of attenuated total reflection Fourier transform infrared (ATR/FT-IR) spectrometry for investigation of bacterial biofilms (7, 26, 29, 30, 35, 36, 46). In the present study this technique was utilized to monitor penetration of a fluoroquinolone antibiotic, ciprofloxacin, to the base of *Pseudomonas aeruginosa* biofilms. Interactions between biofilm biomass constituents and ciprofloxacin were also evaluated. In addition, biofilm morphology was examined and colony forming abilities of treated and untreated biofilm cells were determined.

MATERIALS AND METHODS

Materials. *P. aeruginosa* ERC-1 was obtained from the Center for Biofilm Engineering culture collection (Montana State University, Bozeman, Mont.). This strain was known from previous studies to colonize germanium substrata, forming a relatively confluent biofilm in 24 to 48 h. The composition of the medium used for culturing planktonic and biofilm bacteria was as follows: 0.28 g of D-glucose, 0.017 g of $CaCl_2$, 0.24 g of NH_4Cl, 0.051 g of $MgSO_4 \cdot 7H_2O$ 1.0 g of K_2HPO_4 (anhydrous), and 0.6 ml of Wolfe's mineral salts solution per liter of water (pH 7.1 to 7.2). Water was purified by ion exchange followed by ultrafiltration. Concentrated solutions of glucose and $CaCl_2$, as well as Wolfe's mineral salts solution, were filter sterilized and added to the balance of the medium, which was sterilized by autoclaving. The composition of Wolfe's mineral salts solution (per liter of water) was as follows: 1.5 g of nitriloacetic acid, 3.0 g of $MgSO_4 \cdot 7H_2O$, 0.5 g of $MnSO_4 \cdot H_2O$, 1.0 g of NaCl, 0.1 g of $FeSO_4 \cdot 7H_2O$, 0.1 g of $CoCl_2 \cdot 6H_2O$, 0.1 g of $CaCl_2$, 0.1 g of $ZnSO_4 \cdot 7H_2O$, 0.01 g of $CuSO_4 \cdot 5H_2O$, 0.01 g of $AlK(SO_4)_2 \cdot 12H_2O$, 0.01 g of H_3BO_3, and 0.01 g of $Na_2MoO_4 \cdot 2H_2O$. All tubing was silicone Masterflex (Cole-Parmer Instrument, Niles, Ill.). Ciprofloxacin (10-mg/ml stock solution) was obtained from Miles Canada (Etobicoke, Canada). Chemicals used for staining and cryosectioning were 5-cyano-2,3-ditolyl tetrazolium chloride (CTC) (Polysciences, Warrington, Pa.), 4′,6-diamidino-2-phenylindole (DAPI) (Sigma, St. Louis, Mo.), and Tissue-Tek OCT compound (Miles, Elkhart, Ill.).

Methods. (i) FT-IR spectrometry. A Perkin-Elmer model 1800 FT-IR spectrophotometer equipped with a liquid-N_2-cooled, medium-range mercury-cadmium-telluride detector (5,000 to 580 cm^{-1}) was used to collect the FT-IR spectra. The flow chamber was a Micro-Circle cell designed to enclose a cylindrical germanium internal reflection element (IRE)

* Corresponding author.

(Spectra Tech, Stamford, Conn.). Germanium IREs were cleaned before each experiment by moderate abrasion with 0.05-μm alumina paste followed by successive sonication in 1.0% Micro cleaning solution, ultrapure water, and 95% ethanol. The Circle cell assembly containing the IRE was sterilized by filling the chamber with 70% ethanol and soaking for 1 h.

Theoretical descriptions of the evanescent field which penetrates from the surface of the IRE are available (25). Briefly, the evanescent field intensity decreases exponentially with distance from the IRE surface such that 95% of the energy is contained within 0.477 μm of a germanium-water interface at 2,000 cm^{-1} and within 1.05 μm at 900 cm^{-1}.

Difference spectra of bacteria were acquired at a relatively high resolution: interferograms were double sided, apodization was a weak Beer-Norton function, and the range was 4,000 to 700 cm^{-1} with an interval of 1 cm^{-1} and nominal resolution of 2.00 cm^{-1}. Difference spectra between the colonized IRE and sterile culture media were flattened by using Perkin-Elmer software with reference points at 1,850 and 950 cm^{-1}. Fifty interferograms were averaged per spectrum. Water vapor bands were removed by subtraction of a pure water vapor spectrum. Fluctuations in intensity of the strong water band at 1,640 cm^{-1} resulted in appearance of this band in the difference spectra. This residual water absorption band was removed by subtracting out a pure water spectrum by using the ratio of areas of the absorption water band centered at 2,120 cm^{-1} as a normalization factor (17). Relatively low resolution spectra were acquired to monitor antibiotic transport to the interfacial region and subsequent washout. The acquisition parameters were the same as for the high-resolution spectra except that the nominal resolution was 16 cm^{-1}, with an interval of 4 cm^{-1} and a range of 2,500 to 900 cm^{-1}, with one interferogram acquired per spectrum. With these parameters, spectra could be acquired every 13.8 s by automating the process via macro software. This was sufficiently fast to monitor the kinetics of penetration. Areas of spectral features were computed for the region bounded by the data curve, and a linear baseline drawn between the two limit points of the integration. Limit points were as follows: amide II band of bacterial protein (Fig. 2 and 3), 1,590 to 1,480 cm^{-1}; bands I and II of ciprofloxacin (Fig. 5 and 6), 1,290 to 1,324 cm^{-1} and 1,250 to 1,290 cm^{-1}, respectively; and bands A to C in Fig. 8, 1,700 to 1,760 cm^{-1}, 1,282 to 1,325 cm^{-1}, and 1,050 to 1,070 cm^{-1}, respectively.

(ii) Flow system. The essential components of the experimental configuration are shown in Fig. 1. The rates of flow through the continuous culture (0.5 ml/min; dilution rate, 0.10 h^{-1}), to the bacterial feed (0.5 ml/min), and through the flow chamber (3.2 ml/min) were controlled independently with Masterflex peristaltic pumps (Cole-Parmer Instrument). Clamps were used in order to shunt bacteria from the continuous culture into the flow chamber or to switch to the culture medium containing the antibiotic. Care was taken to maintain uninterrupted flow during rechanneling. Pulsing in the flow chamber was damped using a T-connection which provided a sterile air space between the flow chamber and the pump. Flow rate was monitored periodically by counting drops in glass break tubes located in the lines. For each experiment, culture medium was transferred aseptically into the antibiotic reservoir from the main reservoir. Thus, culture medium containing the antibiotic was identical to the medium not containing the antibiotic except for the presence of the antibiotic. For treated biofilms the colonized IRE was exposed to 100 μg of ciprofloxacin per ml in sterile culture medium for 21 min and then culture medium containing no antibiotic was reintroduced. Immediately before introduction of the culture medium containing the antibiotic into the Circle cell, a spectrum was acquired. Then, spectra were acquired every 13.8 s for 37 min. Experiments were performed in a temperature-controlled environment at 22 to 23°C.

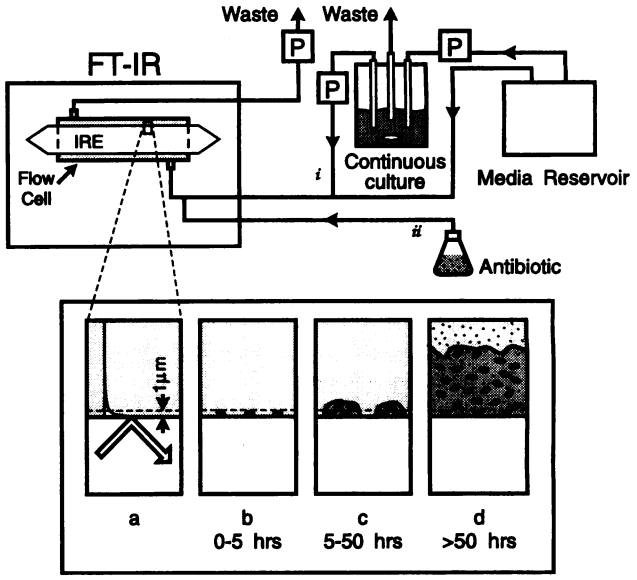

FIG. 1. Schematic representation of the experimental setup. Bacteria from a continuous culture were used to inoculate the flow chamber by opening a clamp (*i*). The antibiotic could be introduced by opening another clamp (*ii*). The cylindrical germanium IRE is shown enclosed in the flow chamber. The enlargement of the interfacial area shows the IR beam reflecting from the interface, producing the exponentially decaying evanescent field (a), cell attachment (b), microcolony formation (c), and mature biofilm with antibiotic penetration (d). Horizontal dashed line, approximate penetration depth of the evanescent field; P, pump.

The volume of the annular region between the Circle cell and the germanium IRE was 0.289 ml; at a flow rate of 3.2 ml/min the residence time was 5.4 s, with a shear rate of 41.5 s^{-1} and a Reynolds number of 9.0 (laminar flow). At a flow rate of 0.505 cm/s the boundary layer for the annular flow chamber bounded by the cylindrical IRE and inner wall of the Circle cell was estimated to be 85 μm (41). The diffusion coefficient of ciprofloxacin through aqueous media, based on the chemical structure, is approximately 4×10^{-6} cm^2/s (44), implying that approximately 20 s is required for the interfacial concentration to reach 90% of its bulk value via diffusion through the boundary layer in aqueous media (13).

(iii) Evaluation of antibiotic efficacy. Standard MICs and MBCs for ciprofloxacin were determined by a broth dilution assay (19).

The colony-forming ability of biofilm cells was evaluated by a standard tube dilution series and plate counts on R2A agar. A portion of the biofilm was removed from the IRE and transferred into dilution broth with a sterile cotton swab. This sample was sonicated for 3 min to break up any cell aggregates and plated. Sonication of this bacterial strain has been shown previously to have no deleterious effect on colony-forming ability on R2A. Cells were DAPI stained and enumerated by direct-count epifluorescence microscopy on polycarbonate membranes (pore size, 0.2 μm; diameter, 25 mm; Nuclepore). In the case of the antibiotic-treated biofilm, the entire surface of the IRE was scraped into the dilution broth with a sterile disposable cell scraper (Fisher Scientific). This was done in

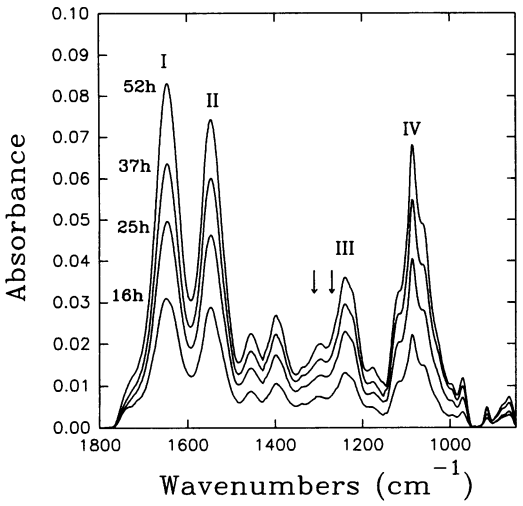

FIG. 2. FT-IR spectra of biofilm bacteria colonizing the surface of the germanium IRE. Spectra were acquired 16, 25, 37, and 52 h after introduction of bacteria to the flow chamber. See Table 1 for identification of prominent spectral features (I to IV). Arrows, positions of bands of the antibiotic spectrum (Fig. 5) which were used to follow transport to the surface.

order to ensure accurate recovery of the anticipated small numbers of viable cells.

(iv) Examination of biofilm morphology. The morphology of thin sections of intact biofilm was examined by means of a cryoembedding technique followed by direct staining (50). The IRE with intact biofilm was immersed in a 0.05% (5 mM) CTC solution in ultrafiltered water for 2 h at 25°C. The CTC solution was then carefully decanted off the IRE and replaced with a 5% formalin solution. Following a 5-min fixation period, the IRE was placed in a 1-μg/ml solution of DAPI for 3 min. The IRE with stained biofilm was cryoembedded in OCT on a dry-ice slab. Sections 5 μm thick were made with a cryostat. Frozen sections were examined by epifluorescence microscopy. CTC staining has been used to measure the respiratory activity of biofilm bacteria (40, 51). Quantitative results obtained in this set of experiments with the CTC labelling technique were inconsistent and are not reported here. The cylindrical surface of the colonized IREs from the 70-h treated biofilm was examined microscopically before biofilm removal.

RESULTS

Lateral colonization of IRE monitored by FT-IR spectrometry. As depicted in Fig. 1, the evanescent field at the interface of the IRE penetrates into the aqueous surrounding medium, sampling an interfacial region approximately 1 μm thick. As bacterial cells attach to the IRE and colonize the surface of the IRE, the IR source radiation is absorbed by components of cells in the first monolayer proximal to the surface. Bands originating from cell components can be clearly distinguished when 5 to 10% of the surface of the IRE is colonized. As bacteria proceed to colonize the surface, these bacterial absorbance bands in the difference spectra increase in intensity (Fig. 2). Similar results have been obtained by others using the ATR/FT-IR methodology (7, 35, 36). Biopolymer groups whose vibrational modes are major contributors to prominent features in the bacterial difference spectrum (Fig. 2) are identified in Table 1.

By monitoring the area of a selected band(s) in the bacterial difference spectra (Fig. 2), it is possible to follow the lateral colonization of the IRE by the bacteria. Figure 3 presents the area of the amide II band versus time for four experiments. For experiments depicted in Fig. 3c and d, ciprofloxacin was introduced at 50 h. Note that in Fig. 3d loss of some interfacial cells is indicated by the reduction in the amide II band. This apparent detachment of interfacial cells became most pronounced about 10 h after reintroduction of the culture medium containing no antibiotic.

TABLE 1. Biopolymers contributing to prominent spectral features

Feature(s)[a]	Cell component(s)	Reference(s)
I and II	Protein (amide I and II)	5, 27, 32
III	RNA and DNA[b] (antisymmetric motion, phosphodiester linkage)	43
IV	RNA and DNA (symmetric motion, phosphodiester linkage[c]), carbohydrates (complex ring vibrations[d])	8, 9, 37, 43

[a] Indicated in Fig. 2.
[b] Weak vibrational modes associated with protein secondary structure (amide III) appear between 1,200 and 1,300 cm^{-1} (23, 24, 38).
[c] Vibrational modes are probably coupled to ribose ring vibrations.
[d] For more specific assignments, see the indicated references.

Biofilm morphology and antibiotic efficacy. The MIC for ciprofloxacin was <0.5 μg/ml; the MBC concentration for the standard test was 1 μg/ml. These are typical values reported for *P. aeruginosa* and ciprofloxacin in clinical settings.

For 50-h experiments (Fig. 3a and c) the colony-forming abilities of the treated and untreated biofilm bacteria were assessed and compared (see "Methods"). For untreated biofilm cells (Fig. 3a) 74% of the total cells recovered from the IRE produced colonies on R2A agar plates. For the treated biofilm cells (Fig. 3c) this percentage dropped to 0.38% (4.0×10^6 CFU/cm^2). This assay was performed for cells recovered from the entire IRE.

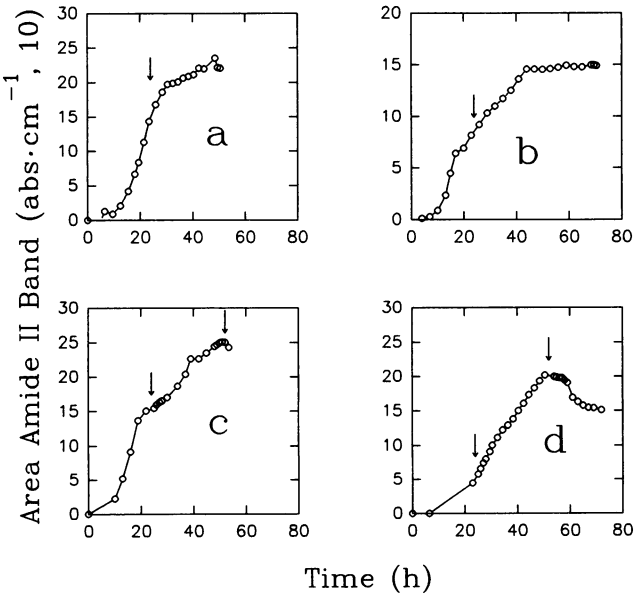

FIG. 3. Lateral colonization of the surface of the germanium IRE monitored by the area of the amide II band (1,590 to 1,480 cm^{-1}) for four experiments (a to d). Time zero corresponds to the introduction of bacteria into the flow chamber. Arrows, termination of bacterial feed (24 h) and exposure to the antibiotic pulse (50 h [c and d]).

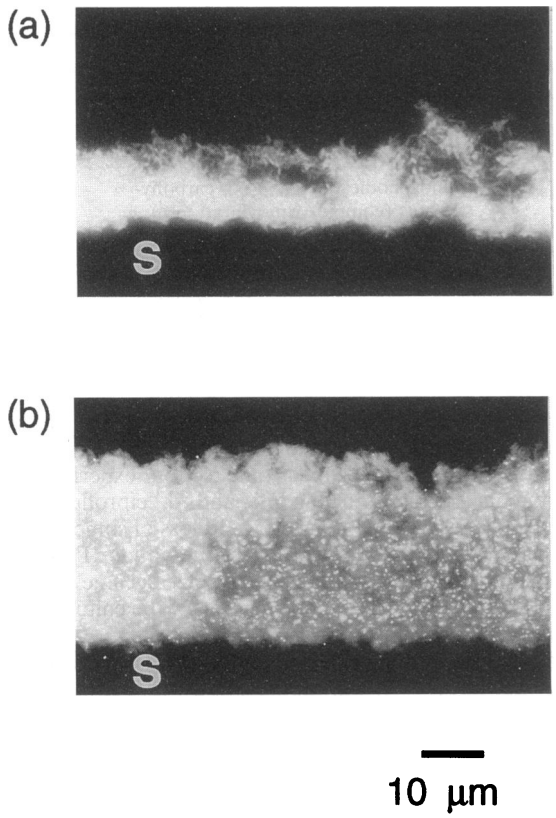

FIG. 4. Epifluorescence micrographs of frozen cross sections of the biofilm treated with ciprofloxacin (a) and untreated biofilm (b). All samples were from 70-h experiments. S, biofilm-substratum interface.

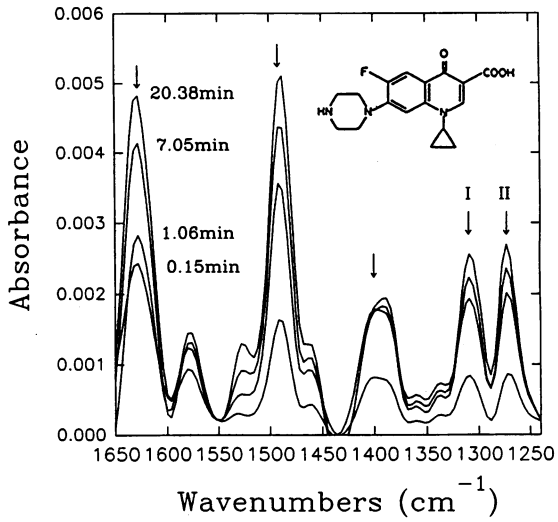

FIG. 5. FT-IR spectra of ciprofloxacin (100 μg/ml in culture medium) showing increase in spectral bands as the antibiotic is delivered to the surface of a sterile (uncolonized) germanium IRE. Spectra were taken at 0.15, 1.06, 7.05, and 20.38 min after a plug of the antibiotic-containing medium entered the flow chamber. Arrows, prominent bands. Bands I and II were used to follow transport of the antibiotic to the base of the biofilm. The structure of ciprofloxacin is indicated.

For the 70-h experiments (Fig. 3b and d) and one 50-h experiment (untreated biofilm, Fig. 3a), biofilm morphology was examined by epifluorescence microscopy of thin film sections of portions of the biofilm which had been removed from the IRE (Fig. 4).

The coverage of the IREs by the biofilm based on epifluorescence microscopic examination of the cylindrical surface (not shown in Fig. 4) was fairly confluent, rather than patchy, even for the 70-h experiment (treated biofilm), in which some detachment of interfacial cells was indicated by the ATR/FT-IR results (Fig. 3d). The average thickness of antibiotic-treated biofilms (70-h experiment) obtained by measuring micrographs of cryosections with a micrometer was 15.1 ± 6.2 μm, whereas the thickness of the untreated biofilm (50- and 70-h experiments combined) was 27.1 ± 8.2 μm. This indicates that the antibiotic treatment induced some detachment of biofilm cells. Representative micrographs of thin film sections of the 50-h untreated and treated *P. aeruginosa* biofilms are shown in Fig. 4.

FT-IR monitoring of antibiotic transport to the base of the biofilm. Figure 5 presents FT-IR spectra of ciprofloxacin (100 μg/ml in sterile culture medium) as it was introduced into a Circle cell containing a sterile IRE. The increase in absorption bands reflects the increase in the interfacial concentration of the antibiotic within the evanescent field. The spectral region containing the most prominent bands of ciprofloxacin is shown. Features of this region which could be readily recognized in spectra obtained during initial antibiotic penetration into the biofilms are indicated by arrows. The bands at 1,303 and 1,270 cm^{-1}, indicated by Roman numerals in Fig. 5 were chosen for monitoring transport of the antibiotic to the base of the biofilm. These relatively pronounced bands overlap less conspicuously than other bands with features of the bacterial spectrum (Fig. 2).

Figure 6 presents spectra acquired from an IRE colonized for 50 h and exposed to the antibiotic. The spectra presented are difference spectra between a bacterial spectrum acquired immediately before introduction of the antibiotic into the Circle cell and subsequent spectra acquired at specified times after ciprofloxacin (100 μg/ml) was introduced into the Circle cell. Bands associated with the antibiotic are indicated by arrows (compare Fig. 5 and 6). Troughs in the spectra which appeared at approximately 1,500 cm^{-1}, along the two edges of the range displayed, and for later times, at approximately 1,400 and 1,450 cm^{-1} are the result of decreases in the bands of the (background) bacterial spectrum during exposure to the antibiotic, presumably caused by detachment of interfacial cells.

Figures 7a to d present areas of two selected bands of the FT-IR spectrum of ciprofloxacin (Fig. 5 and 6) versus time for the 21 min during which the antibiotic pulse was flowing through the Circle cell and for a subsequent 16 min after reintroduction of the sterile culture medium containing no antibiotic. Each of the figures presents data from two experiments. Data from sterile and colonized IREs are presented in Fig. 7a and b and Fig. 7c and d, respectively. For the colonized IREs (Fig. 7c and d) the lateral growth curves are presented in Fig. 3c and d.

Qualitative interpretation of the time course data curves. A comparison of Fig. 7a and b with Fig. 7c and d reveals that the time course of transport and removal of the antibiotic to and from the interfacial region of the IRE was significantly affected by the presence of the *P. aeruginosa* biofilm. After reintroduction of culture medium without the antibiotic, the antibiotic was rinsed nearly completely from the surface of the sterile IRE during the 16-min washout period; in the case of the colonized IRE, a substantial amount of the antibiotic was still contained in the interfacial region. In addition, the time course

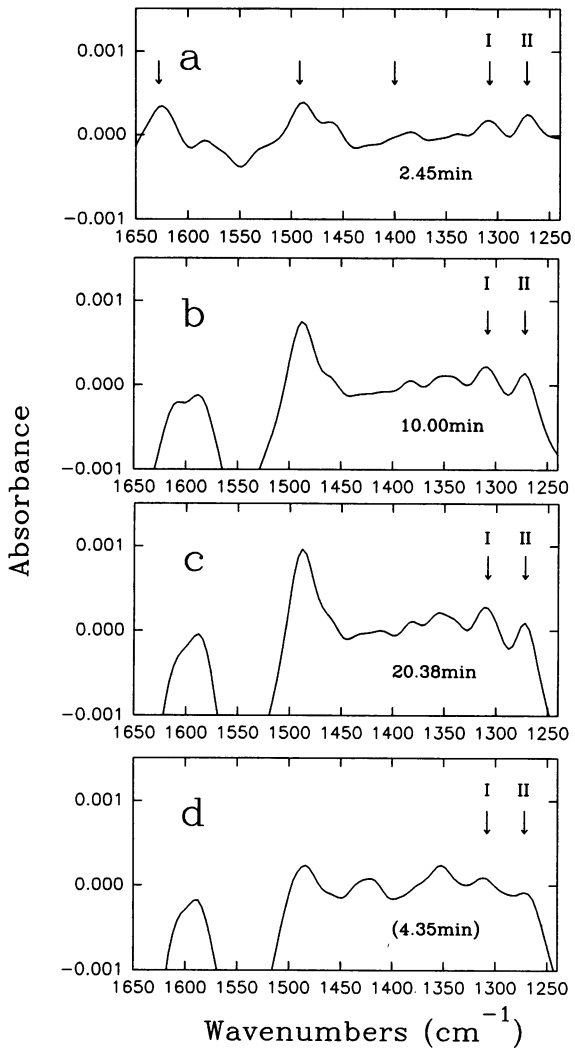

FIG. 6. Transport of ciprofloxacin to the base of a *P. aeruginosa* biofilm. (a to c) Difference spectra between the bacterial spectrum immediately before the introduction of the antibiotic to the flow chamber and spectra 2.45 min (a) 10.00 min (b), and 20.38 min (c). after the antibiotic entered the flow chamber. Spectrum d was taken 4.35 min after reintroduction of non-antibiotic-containing culture medium. Bands of the antibiotic appear at 1,630, 1,480 (1,462-cm^{-1} shoulder), 1,300, and 1,270 cm^{-1} (compare with Fig. 5). Prominent bands associated with the antibiotic are indicated. I and II, bands used to follow the time course of antibiotic transport into and subsequent washout from the biofilm.

of delivery of the antibiotic to the base of the interfacial region was altered by interaction with the biofilm. In Fig. 7c and d the time courses for delivery to the sterile IRE are replotted along with the time courses for the colonized IRE. It is evident from a comparison of the shapes of the curves that the rate of transport to the surface of the colonized IRE was reduced compared with that for the sterile IRE. The areas under the bands indicate that the final interfacial concentration for the sterile IRE was four to five times higher than that for the colonized IRE at the end of the 21-min dose period.

Quantitative analysis of the time course data curves. Figure 7e is a semilog plot of data presented in Fig. 7a for antibiotic delivery to a sterile IRE. Abscissa values consist of a simple manipulation of the datum point values as indicated on the axis of Fig. 7e and described below (equation 1). The curve consists of two sections: an initial period of three or four time points (40 to 50 s) in which the curve is steeply sloping and nonlinear and a later section, which is less sloping and fairly linear in the semilog plot. Approximately 10 s is required for the antibiotic to reach the entrance of the flow chamber from the Y connection in Fig. 1. An additional 5 s is needed for the antibiotic to flood the flow chamber once it has reached the entrance, and approximately 20 s is required for diffusion through the boundary layer. Thus, 90% of the antibiotic should have reached the interfacial region of a sterile IRE within about 30 to 40 s. It seems likely that the earlier, more steeply sloping (nonlinear) section of the curve presented in Fig. 7e is the result of relatively rapid diffusion into the interfacial region through the boundary layer (requiring about 30 to 40 s, as outlined above). The later, less steeply sloping section can be attributed to a slower first-order process, namely, adsorption onto the surface of the IRE.

The time course curves for transport to the surface of the colonized IRE can be fit fairly accurately with a simple analytical model quite different from that for the sterile IRE. Figure 7g presents a replot of data presented in Fig. 7c versus the square root of time ($t^{1/2}$). The curves can be fit quite well with a straight line. Correlation coefficients for fits to data presented in Fig. 7c and d, replotted in terms of $t^{1/2}$, are 0.96873, 0.99084, 0.99095, and 0.99096. This linearity with respect to $t^{1/2}$ is not found for the time course of delivery to the surface of the sterile IRE (Fig. 7f), where a first-order adsorption process dominates at later times (Fig. 7e).

In order to estimate the concentration of the antibiotic penetrating into the interfacial region, a standard curve was constructed. For antibiotic concentrations of 50, 100, 200, and 400 μg/ml, transport to a sterile IRE was monitored and a set of curves similar to those presented in Fig. 7a and b was obtained. By using nonlinear regression, the curves for later times (>50 s) were each fit as follows:

$$\text{data}(t) = s[1 - \exp(-kt)] + c \quad (1)$$

where s, k, and c are the fitted parameters and t is time. The parameter c gives an estimate of the contribution to the data curve resulting from rapid diffusion into the interfacial region with negligible adsorption. A graphic method for obtaining approximately the same values is to replot the data as ln (1 − data(t)/P), where P is the estimated plateau value (for long times). The change in interfacial concentration resulting from initial rapid diffusion can then be estimated from the point at which the curve becomes linear on the semilog plot. This type of plot is presented in Fig. 7e, in which the ordinate axis symbol D stands for data$_t$. The result of plotting parameter c (equation 1) versus the concentration of the antibiotic introduced into the flow chamber is presented in Fig. 7h. The curve is fairly linear for lower concentrations, but at higher concentrations the absorption falls off, failing to satisfy Beer's law. By using the linear portion of the curve presented in Fig. 7h for calibration, the interfacial concentration of the antibiotic delivered to the surface of the colonized IRE after a 21-min exposure was estimated to be between 29 and 70 μg/ml (29 and 70% of the bulk concentration introduced into the flow chamber, respectively). These estimates are based on the areas of bands I and II of the antibiotic, respectively. The sloping baseline for later time points may have resulted in an overestimation based on areas of band II (Fig. 6).

Appearance of new spectral features in the treated biofilm. A comparison of spectra from treated and untreated biofilms in the 70-h experiments reveals that changes caused by inter-

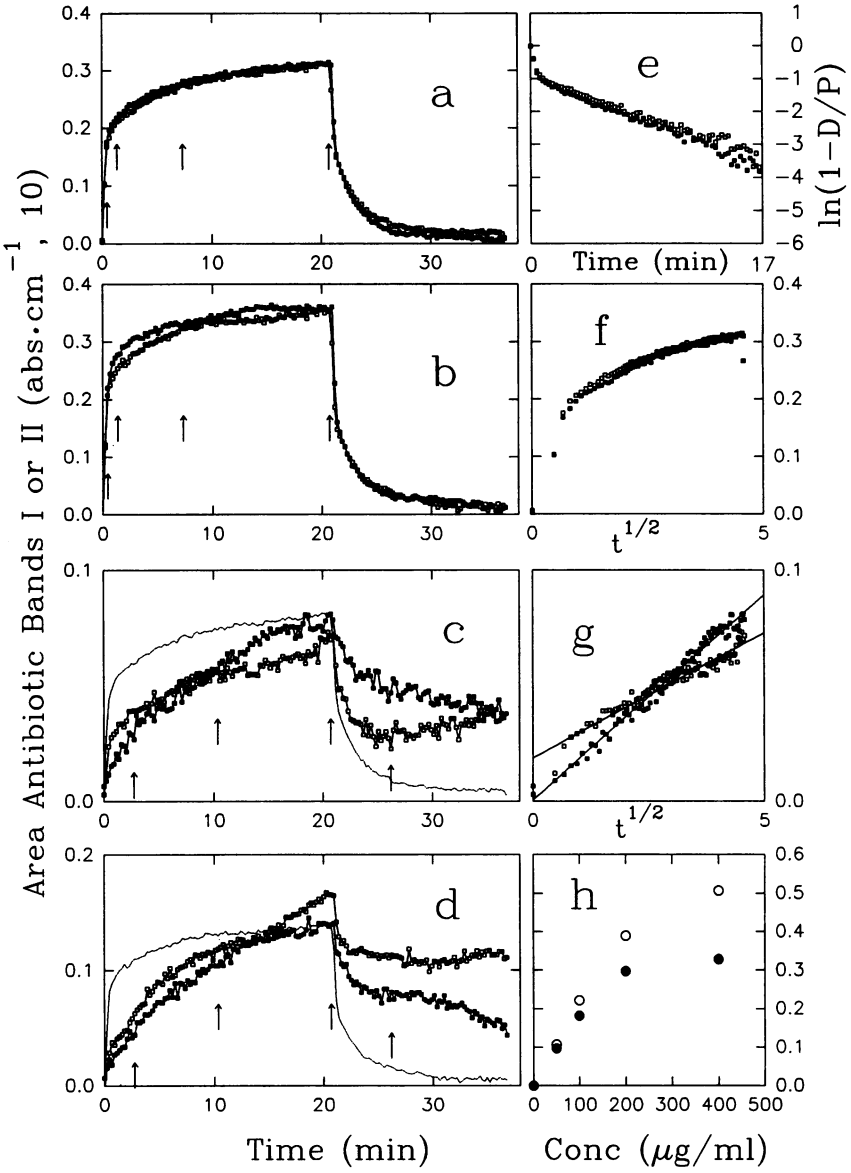

FIG. 7. (a to d) Time courses of transport of the antibiotic to the surface of a sterile germanium IRE (a and b) and an IRE colonized by a *P. aeruginosa* biofilm (c and d) and washout after reintroduction of non-antibiotic-containing culture media, as monitored by the areas under bands I (a and c) and II (b and d) as specified in Fig. 5 and 6. Each panel presents the results of two separate experiments. Solid lines in panels c and d, normalized replotting of time courses for a sterile IRE to aid in shape comparison. Arrows, times of spectra in Fig. 5 and 6. (e) Semilog plot of the delivery period in panel a (see the text for the exact data manipulation); (f) replot of the delivery period of panel a in terms of $t^{1/2}$; (g) replot of the delivery period of panel c in terms of $t^{1/2}$ with regression lines drawn; (h) areas of band I (closed circles) and band II (open circles) contributed primarily by rapid diffusion into the interfacial region of a sterile IRE, with relatively small contribution from adsorption (as determined from equation 1) versus concentration of ciprofloxacin in the bulk fluid.

action with the antibiotic occurred in the bacterial spectra (Fig. 8). Three distinct features or bands began appearing after the reintroduction of culture medium containing no antibiotic, and these bands continued to become more pronounced for the subsequent 20 h of the experiment. These changes did not appear in the spectra of the 70-h untreated biofilm (Fig. 8). It is unlikely that the spectral changes indicated in Fig. 8 are the result of the signal directly from the residual antibiotic which remained in the biofilm. The bands continued to increase hours after the washout period, and after 20 h the band areas were 2 to 15 times larger than the most prominent bands in the antibiotic spectrum at the end of the 21-min pulse period (i.e., the point at which the maximum absorbance from the penetrating antibiotic was measured). Therefore, the spectral changes were most likely produced in the bacterial biofilm through interaction with the antibiotic which was either entrapped within the extracellular polymeric substances or contained within the cells.

DISCUSSION

Transport of the antibiotic to the base of the biofilm. The data for the time course of appearance of the antibiotic (Fig. 7) imply that transport from the bulk medium to the interfacial

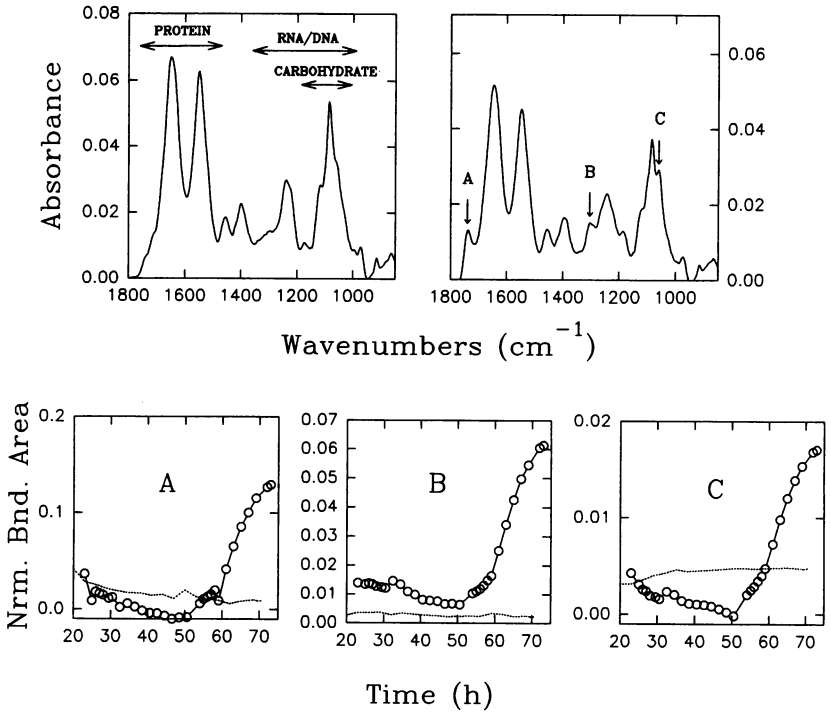

FIG. 8. Changes in the bacterial spectrum produced by interaction with the antibiotic. (Upper panels) Bacterial spectra immediately before the introduction of the antibiotic (upper left) and 20 h after the introduction (upper right). Approximate regions of strong absorption bands of the three bacterial biopolymer groups are indicated (upper left). Time courses of areas of spectral features A to C are plotted below. Dotted curves, changes produced in these spectral regions in the untreated biofilm. Areas have been normalized to the area of the amide II band.

region was nearly complete after 40 s for a sterile (uncolonized) IRE. An argument that adsorption onto the surface was primarily responsible for the increase in the FT-IR absorption bands of the antibiotic at times after 40 s (Fig. 7a and b) was presented. This increase was approximately first order. In contrast, the transport of the antibiotic to the surface of the colonized IRE can be described by a time course which is nearly linear with respect to $t^{1/2}$. Linearity with respect to $t^{1/2}$ is usually interpreted as an indication of diffusion-limited transport (1). During this time interval the antibiotic in this interfacial region reached between 29 and 70% of the concentration in the bulk medium. The data indicate incontrovertibly that the biofilm was much less permeable to the antibiotic than an aqueous solution.

If the biofilm is conceptualized as a homogeneous film having a uniform thickness and a uniform density, an effective diffusion coefficient for transport to the interfacial region can be estimated. For a film with this simple geometry, transport to the interface can be described approximately by a time course curve which, after a delay, rises linearly with respect to the square root of time until the surface has reached about 75% of the bulk concentration and then falls off to a plateau (13). On the basis of this simple model, the slopes of data curves for antibiotic penetration in Fig. 7c and d plotted against $t^{1/2}$ can be used to estimate an effective diffusion coefficient of between 1.5×10^{-10} and 9×10^{-10} cm^2/s for penetration of the antibiotic into the biofilm. (The range of values originates from the uncertainty in the interfacial concentration and the range in slopes of the data curves versus $t^{1/2}$.) However, the estimated delay for the appearance of the antibiotic at the interface, according to this simple model, should be between 87 and 522 s for the diffusion coefficients calculated and a film thickness of 20 μm.

The results suggest that a limited quantity of the antibiotic was delivered rapidly to a small portion of the colonized interface while the remainder of the interfacial region was accessible to the antibiotic only via more circuitous or impeded avenues. The sum total of these processes resulted in a relation for the time course of transport which was approximately linear with respect to $t_{1/2}$. The transport of a chemical substance through a biofilm can probably occur by various pathways. By using confocal scanning laser microscopy, pores or channels which permeate biofilms composed of various bacterial species have been observed (14). For a reactive substance, such as an antibiotic, entrapment and modification (or, in some cases, consumption) must also be considered.

The curves for antibiotic removal from the interface of the colonized IRE (Fig. 7c and d) provide evidence that the antibiotic was being entrapped within the biofilm. If the antibiotic was binding to biofilm components (extracellular polymeric substances, cell envelope, etc.), this may explain the extremely impeded transport to certain portions of the biofilm, which is reflected in the minute effective diffusion coefficient given above. The rate of transport would in this case be regulated by the relative rates of adsorption to and desorption from the various biofilm components and not by diffusion in the strict sense.

Various explanations have been proposed to account for the recalcitrance of biofilm bacteria to antibiotics which has been observed repeatedly in situ (2–4, 33, 34). Transport limitations may be so extreme that bacteria in certain portions of the biofilm are exposed to less than the biocidal dose of the antibiotic during a treatment course. In cases in which transport is less drastically altered, penetration of the antibiotic to certain portions of the biofilm may be delayed, allowing bacteria time to induce production of resistance factors. Alter-

natively, it is possible that the biofilm cells have some inherent resistance which their planktonic counterparts are lacking and that transport limitations play a minor role. The correct appraisal of the factors limiting efficacy against biofilm bacteria can have profound implications for appropriate design of antimicrobial agents. The data presented here demonstrate that a relatively thin biofilm (15 to 30 μm) can significantly impede transport of an antimicrobial agent from the bulk medium to the interfacial region. After this exposure period a significant number (4×10^6 CFU/cm^2) of viable cells were recovered from the biofilm. Therefore, delay in delivery to a portion of the biofilm population and/or inaccessibility of portions of the biofilm population should be seriously considered as possible factors contributing to the diminished efficacy of antimicrobial agents toward biofilm bacteria.

Interpretation of changes appearing in the bacterial spectrum. The appearance of the three bands or shoulders identified in Fig. 8 was synchronous, implying that they originated from the same set of chemical interactions or, perhaps, even from the same interaction. Transition from the A form of DNA to the B form (15, 42) produces similar changes in the IR spectrum (43). Ciprofloxacin is a DNA gyrase inhibitor which is known to result in double-stranded nicks in DNA (49) and, therefore, may grossly perturb the secondary structure as well. It is possible that the spectral changes were the result, directly, of the action of the antibiotic. On the basis of studies in which relative quantities of biomass components have been determined for various bacterial species under a range of growth conditions (28, 31, 39), it is likely that the cellular quantity of DNA in biofilms exceeds that required so that gross changes in the DNA spectrum could be detected on top of the other interfering bands (i.e., primarily bands arising from RNA). If the changes in the FT-IR spectra indicated in Fig. 8 represent a direct spectroscopic observation of changes produced specifically by the action of the DNA gyrase inhibitor ciprofloxacin, this would provide an in situ methodology for monitoring antimicrobial action in biofilms. The definitive set of corroborative experiments would involve in vitro FT-IR assays of the interaction between the antibiotic and isolated bacterial DNA.

ACKNOWLEDGMENTS

This work was supported by Miles Canada, cooperative agreement ECD-8907039 between the National Science Foundation and Montana State University, Electrical Power Research Institute grant RP8011-2, and Office of Naval Research grant N00014-93-1-0168.

We thank Gayle Callis for performing the cryosectioning.

REFERENCES

1. **Andrade, J. D.** 1985. Principles of protein adsorption, p. 1–80. *In* J. D. Andrade (ed.), Surface and interfacial aspects of biomedical polymers, vol. 2. Protein adsorption. Plenum Press, New York.
2. **Anwar, H., T. Biesen, M. Dasgupta, K. Lam, and J. W. Costerton.** 1989. Interaction of biofilm bacteria with antibiotics in a novel chemostat system. Antimicrob. Agents Chemother. **33:**1824–1826.
3. **Anwar, H., and J. W. Costerton.** 1990. Enhanced activity of combination of tobramycin and piperacillin for eradication of sessile biofilm cells of *Pseudomonas aeruginosa*. Antimicrob. Agents Chemother. **34:**1666–1671.
4. **Anwar, H., J. L. Strap, and J. W. Costerton.** 1992. Kinetic interaction of biofilm cells of *Staphylococcus aureus* with cephalexin and tobramycin in a chemostat system. Antimicrob. Agents Chemother. **36:**890–893.
5. **Bandekar, J., and S. Krimm.** 1980. Vibrational analysis of peptides, polypeptides, and proteins. VI. Assignment of β-turn modes in insulin and other proteins. Biopolymers **19:**31–36.
6. **Bisno, A. L., and F. A. Waldvogel.** 1989. Introduction, p. 1–2. *In* A. L. Bison and F. A. Waldvogel (ed.), Infections associated with indwelling medical devices. American Society for Microbiology, Washington, D.C.
7. **Bremer, P. J., and G. G. Geesey.** 1991. An evaluation of biofilm development utilizing non-destructive attenuated total reflectance Fourier transform infrared spectroscopy. Biofouling **3:**89–100.
8. **Cael, J. J., K. H. Gardner, J. L. Koenig, and J. Blackwell.** 1975. Infrared and raman spectroscopy of carbohydrates. Paper V. Normal coordinate analysis of cellulose I. J. Chem. Phys. **62:**1145–1153.
9. **Cael, J. J., J. L. Koenig, and J. Blackwell.** 1975. Infrared and raman spectroscopy of carbohydrates. Paper VI. Normal coordinate analysis of V-amylose. Biopolymers **14:**1885–1903.
10. **Christensen, G. D., L. M. Baddour, D. L. Hasty, G. H. Lowrance, and W. A. Simpson.** 1989. Microbial and foreign body factors in the pathogenesis of medical device infections, p. 27–59. *In* A. L. Bison and F. A. Waldvogel (ed.), Infections associated with indwelling medical devices. American Society for Microbiology, Washington, D.C.
11. **Costerton, J. W., K.-J. Cheng, G. G. Geesey, T. I. Ladd, J. C. Nickel, M. Dasgupta, and T. J. Marrie.** 1987. Bacterial biofilm in nature and disease. Annu. Rev. Microbiol. **41:**435–464.
12. **Costerton, J. W., T. J. Marrie, and K.-J. Cheng.** 1985. Phenomena of bacterial adhesion, p. 3–43. *In* D. C. Savage and M. M. Fletcher (ed.), Bacterial adhesion: mechanisms and physiological significance. Plenum Press, New York.
13. **Crank, J.** 1956. The mathematics of diffusion, p. 42–61. Oxford University Press, London.
14. **DeBeer, D., P. Stoodley, F. Roe, and Z. Lewandowski.** 1993. Oxygen distribution and mass transport in biofilms. Biotechnol. Bioeng. **43:**1131–1138.
15. **Dickerson, R. E., M. L. Kopka, and H. R. Drew.** 1983. Structural correlations in B-DNA, p. 149–179. *In* E. Clementi and R. H. Sarma (ed.), Structure and dynamics: nucleic acids and proteins. Adenine Press, New York.
16. **Dickinson, G. M., and A. L. Bisno.** 1989. Infections associated with indwelling devices: infections related to extracellular devices. Antimicrob. Agents Chemother. **33:**602–607.
17. **Dousseau, F., M. Therien, and M. Pezolet.** 1989. On the spectral subtraction of water from FTIR spectra of aqueous solutions of proteins. Appl. Spectrosc. **43:**538–542.
18. **Evans, D. J., D. G. Allison, M. R. W. Brown, and P. Gilbert.** 1991. Susceptibility of *Pseudomonas aeruginosa* and *Escherichia coli* biofilms towards ciprofloxacin: effect of specific growth rate. J. Antimicrob. Chemother. **27:**177–184.
19. **Gerhardt, P.** 1981. Manual of methods for general bacteriology. American Society for Microbiology, Washington, D.C.
20. **Giwercman, B., E. T. Jensen, N. Hoiby, A. Kharazmi, and J. W. Costerton.** 1991. Induction of β-lactamase production in *Pseudomonas aeruginosa* biofilms. Antimicrob. Agents Chemother. **35:**1008–1010.
21. **Gristina, A. G.** 1987. Biomaterial-centered infection: microbial adhesion vs. tissue integration. Science **237:**1588–1595.
22. **Hoyle, B. D., J. Jass, and J. W. Costerton.** 1990. The biofilm glycocalyx as a resistance factor. J. Antimicrob. Chemother. **26:**1–5.
23. **Jakobsen, R. J., and F. M. Wasacz.** 1987. Effects of the environment on the structure of adsorbed proteins: FTIR studies, p. 339–361. *In* J. L. Brash and T. A. Horbett (ed.), Proteins at interfaces: physiochemical and biochemical studies. American Chemical Society, Washington, D.C.
24. **Kaiden, K., T. Matsui, and S. Tanaka.** 1987. A study of the amide III band by FT-IR spectrometry of the secondary structure albumin, myoglobin and γ-globulin. Appl. Spectrosc. **41:**180.
25. **Knutzen, K., and D. J. Lyman.** 1985. Surface infrared spectroscopy, p. 197–247. *In* J. D. Andrade (ed.), Surface and interfacial aspects of biomedical polymers, vol. 1. Surface chemistry and physics. Plenum Press, New York.
26. **Mittelman, M. W., D. E. Nivens, C. Low, and D. C. White.** 1990. Differential adhesion, activity, and carbohydrate: protein ratios of *Pseudomonas atlantica* monocultures attaching to stainless steel in a linear shear gradient. Microb. Ecol. **19:**269–278.
27. **Miyazawa, T., and E. R. Blout.** 1961. The infrared spectra of polypeptides in various conformations: amide I and II bands. J. Am. Chem. Soc. **83:**712–719.

28. **Moyer, C. L., and R. Y. Morita.** 1989. Effect of growth rate and starvation-survival on cellular DNA, RNA, and protein of a psychrophilic marine bacterium. Appl. Environ. Microbiol. **55:** 2710–2716.
29. **Naumann, D., D. Helm, and H. Labischinski.** 1991. Microbiological characterization by FT-IR spectroscopy. Nature (London) **351:**81–82.
30. **Naumann, D., D. Helm, H. Labischinski, and P. Giesbrecht.** 1991. The characterization of microorganisms by Fourier-transform infrared spectroscopy (FTIR), p. 43–96. *In* W. H. Nelson (ed.), Modern techniques for rapid microbiological analysis. VCH Publishers, New York.
31. **Neidhardt, F. C., J. L. Ingraham, and M. Schaechter.** 1990. Physiology of the bacterial cell, a molecular approach, p. 4. Sinauer Associates, Inc., Sunderland, Mass.
32. **Nevskaya, N. A., and Y. N. Chirgadze.** 1976. Infrared spectra and resonance interactions of amide-I and II vibrations of α-helix. Biopolymers **15:**637–648.
33. **Nickel, J. C., and J. W. Costerton.** 1992. Bacterial biofilms and catheters: a key to understanding bacterial strategies in catheter-associated urinary tract infections. Can. J. Infect. Dis. **3:**261–267.
34. **Nickel, J. C., I. Ruseska, J. B. Wright, and J. W. Costerton.** 1985. Tobramycin resistance of *Pseudomonas aeruginosa* cells growing as a biofilm on urinary catheter material. Antimicrob. Agents Chemother. **27:**619–624.
35. **Nivens, D. E., J. Q. Chambers, T. R. Anderson, A. Tunlid, and D. C. White.** 1993. Monitoring microbial adhesion and biofilm formation by attenuated total reflection/Fourier transform infrared spectroscopy. J. Microbiol. Methods **17:**199–213.
36. **Nivens, D. E., J. Schmit, J. Sniatecki, T. Anderson, J. Q. Chambers, and D. C. White.** 1993. Multichannel ATR/FT-IR spectrometer for on-line examination of microbial biofilms. Appl. Spectrosc. **47:**668–671.
37. **Parker, F. S.** 1983. Applications of infrared, raman, and resonance raman spectroscopy in biochemistry, p. 315–347. Plenum Press, New York.
38. **Pitt, W. G., S. H. Spiegelberg, and S. L. Cooper.** 1987. Adsorption of fibronectin to polyurethane surfaces: Fourier transform infrared spectroscopic studies, p. 324–338. *In* J. L. Brash and T. A. Horbett (ed.), Proteins at interfaces: physiochemical and biochemical studies. American Chemical Society, Washington, D.C.
39. **Poulsen, L. K., G. Ballard, and D. A. Stahl.** 1993. Use of rRNA fluorescence in situ hybridization for measuring the activity of single cells in young and established biofilms. Appl. Environ. Microbiol. **59:**1354–1360.
40. **Rodriguez, G. G., D. Phipps, K. Ishiguro, and H. F. Ridgway.** 1992. Use of a fluorescent redox probe for direct visualization of actively respiring bacteria. Appl. Environ. Microbiol. **58:**1801–1808.
41. **Ross, T. K., and A. A. Wragg.** 1965. Electrochemical mass transfer in annuli. Electrochem. Acta **10:**1093–1106.
42. **Sarma, R. H.** 1980. Is DNA really a double helix? Its diverse spatial configurations and the evidence for a vertically stabilized double helix, p. 83–108. *In* R. H. Sarma (ed.), Nucleic acid geometry and dynamics. Pergamon Press, New York.
43. **Taillandier, E., J. Liquier, and J. A. Taboury.** 1985. Infrared spectral studies of DNA conformations, p. 65–114. *In* R. J. H. Clark and R. E. Hester (ed.), Advances in infrared and raman spectroscopy, vol. 12. John Wiley and Sons, New York.
44. **Treybal, R. E.** 1981. Mass transfer operations, p. 35. McGraw-Hill Book Company, London.
45. **Valeur, A., A. Tunlid, and G. Odham.** 1988. Differences in lipid composition between free-living and initially adhered cells of a Gram-negative bacterium. Arch. Microbiol. **149:**521–526.
46. **van der Mei, H. C., J. Noordmans, and H. Busscher.** 1989. Molecular surface characterization of oral streptococci by Fourier transform infrared spectroscopy. Biochim. Biophys. Acta **991:**395–398.
47. **Ward, K. H., M. E. Olson, K. Lam, and J. W. Costerton.** 1992. Mechanism of persistent infection associated with peritoneal implants. J. Med. Microbiol. **36:**406–413.
48. **Wimpenny, J. W. T., and S. L. Kinniment.** 1992. Measurement of the contribution of adenylate concentrations and adenylate charge across *Pseudomonas aeruginosa* biofilms. Appl. Environ. Microbiol. **58:**1629–1635.
49. **Wolfson, J. S., and D. C. Hooper (ed.).** 1989. Quinolone antimicrobial agents, p. 5–34. American Society for Microbiology, Washington, D.C.
50. **Yu, F. P., G. M. Callis, P. S. Stewart, T. Griebe, and G. A. McFeters.** Cryosectioning of biofilms for microscopic examination. Biofouling, in press.
51. **Yu, F. P., and G. A. McFeters.** 1993. Abstr. Gen. Meet. Am. Soc. Microbiol. 1993, Q 74, p. 359.